Journal of Physics: Conference Series

PAPER • **OPEN ACCESS**

Simulation of thrust magnetic bearings for levitation systems

To cite this article: I.V. Anischenko *et al* 2020 *J. Phys.: Conf. Ser.* **1590** 012061

Simulation of thrust magnetic bearings for levitation systems

Anischenko I.V., Pokrovskii S.V., Rudnev I.A.

National Research Nuclear University MEPhI (Moscow Engineering Physics Institute), Kashirskoe sh. 31, 115409 Moscow, Russia

mephizic@gmail.com

Abstract. This work presents the complex results of the FEM H-formulation modeling of the thrust magnetic bearing based on 2G HTS tapes. The simulated bearing consists of the HTS stator and PMs rotor. In the model we have used the magnetic and transport characteristics of industrial $GdBa_2Cu_3O_{7-x}$ superconductors and also took into account the thermal properties of each layer of high-temperature superconducting tape and the features of the layered structure of the whole stack. The numerical simulation was performed using the finite element method. The developed model feature is a direct magnetic assembly rotation simulation. Load characteristics and losses in the system at several operating temperatures were obtained. Comparison with the experimental results was done.

1. Introduction

Non-contact moving power HTS supports and suspensions form the basis of the modern high-speed levitation ground transport. Magnetic HTS supports and bearings can also be used independently, for example, in the kinetic energy storage systems, gyroscopic stabilization devices, motors and generators [1-3]. The choice of a particular magnetic support scheme is determined by the necessary levitation force F_z value, the required damping parameters, the acceptable levitation gap value, cost characteristics, etc. Since the superconductors properties strongly depends on temperature, orientation and the external magnetic field magnitude, cooling and magnetization modes, the numerical simulation taking into account the electrophysical and thermal processes relationship is necessary to solve the non-stationary problem, when the system parameters greatly vary with the time.

FEM modeling is a powerful tool in terms of both: understanding the physical mechanisms in HTS and also predicting the performance of applications based on them, especially for the complex systems, where analytical solutions are not applicable. This paper presents the magnetic bearing with the HTS stator numerical simulation results. The magnetic assembly block consists of 48 permanent magnets stacked on top of each other in three rows of 16 magnets. Each row is magnetized opposite to the neighboring one. The complexity of magnetic systems need to take into account the superconducting materials properties in gradient magnetic fields. Therefore, using the special software taking into account the features of the three-dimensional magnetic system and sharply non-linear hysteresis materials properties is necessary. The HTS stator is a 2G HTS tape wound in 10 layers on a non-conductive shaft and located parallel to the magnetic assembly center. The distance between the HTS block and the magnetic block is 2 mm.

2. Computational model

As it was mentioned earlier, the subject of this study is a magnetic bearing with the HTS stator. The bearing construction and the calculation system geometry are shown in Figure 1. The magnetic bearing stator is a non-conductive shaft, on which a HTS tape is wound in 10 layers. The characteristics of the simulated tape correspond to the characteristics of industrial tapes of SuperOx (Russia) production. The experimentally measured critical current of the tape was 550 A (own field, 77.4 K). In the framework of the model, in addition to the superconducting layer (1 μm), the substrate layers (0.1 mm), copper, and silver (5 μm) are considered. The bearing rotor consists of the permanent magnets arranged in three rows of 16 magnets each. Magnets have the characteristics of magnets of N 42 mark and dimensions of 10 x 10 x 10 mm^3, for which the residual induction on the surface was measured by Hall magnetometry and amounted to 0.15 T. The magnets assembly are stacked on top of each other in three rows. In each row there are 16 magnets, while each adjacent two magnets rows have a counter magnetization directions.

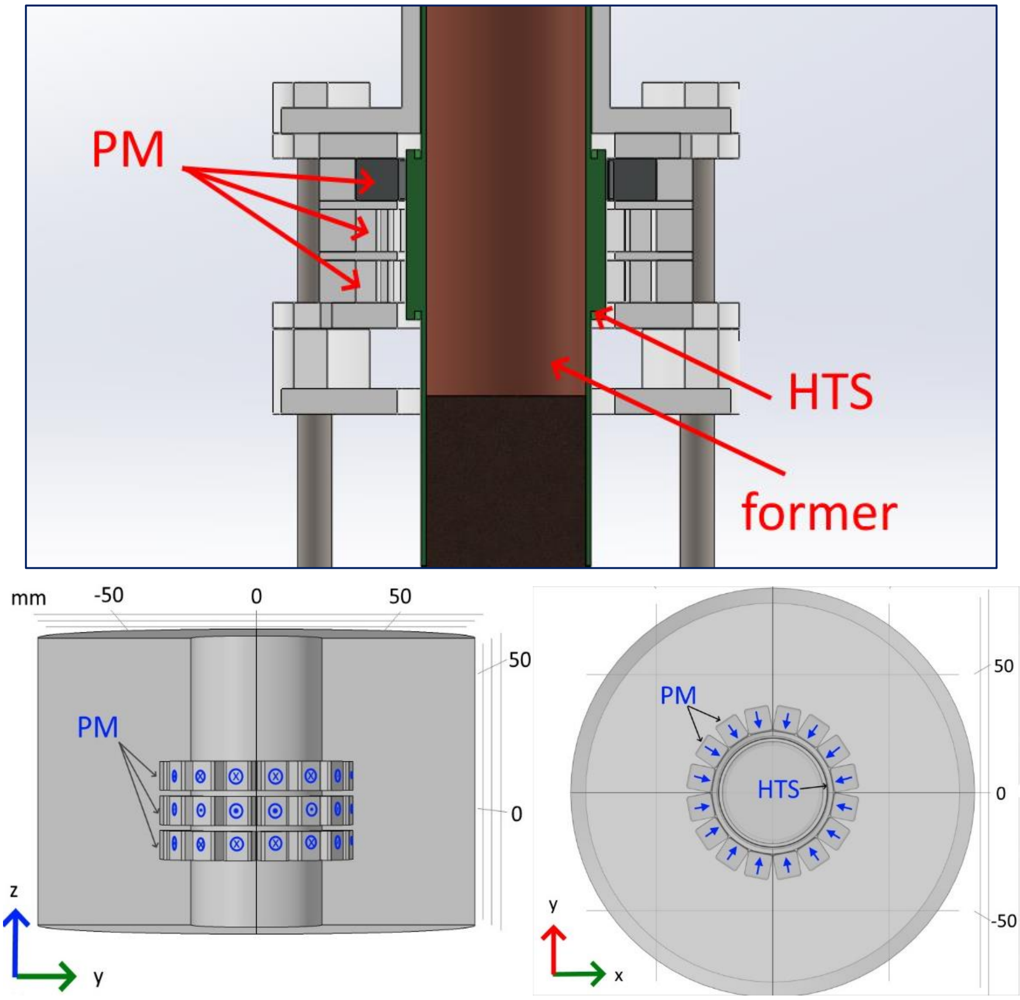

Figure 1. The HTS bearing and the simulated system geometries.

The described system was simulated using the finite element method, which was implemented using the general form of differential equations (PDE) of the Comsol Multiphysics software. The problem was solved in the magnetic field components terms (H-formulation). This approach was previously successfully used by our group to calculate the HTS tapes stacks in the complex gradient fields of the various magnetic assemblies types [4]. The difference in the calculation approach in modeling is only that for the magnetic assembly, it is not the speed of movement along the axis that is specified, but the angular rotation speed with a given frequency. Thus, a distinctive feature of the developed model is the direct modeling of the magnetic field sources motion, which is necessary when calculating complex systems for which external magnetic fields are difficult to analytically determine.

As input parameters, the model uses the experimentally measured angular critical current dependences on the magnetic field, the temperature dependences of the critical current of the HTS layer, the thermal conductivities, and the specific heats of all tape layers. The experimental temperature dependences for all tape layers are introduced into the model in the form of the interpolation [5-12].

In addition, two cooling modes for the superconductor were implemented in the calculations: liquid nitrogen cooling and cryocooler cooling. In the first case, the liquid nitrogen boiling curve hysteretic nature, the possibility of a thermal delay in the onset of bubble boiling, and the multiple changes in the refrigerant boiling modes are taken into account [14–16]. The thermal calculation in this case comes down to determining the effective heat transfer coefficient from a volumetric heat source, which is an HTS tape. These is due to the thermal equilibrium establishing processes and the features of heat removal to liquid nitrogen when changing the boiling regimes (from convective to bubbling and conversely). In the liquid nitrogen case, the hysteretic character of the LN_2 boiling curve and the presence of an additional thermal delay of bubble boiling onset (overheating) play an important role in thermal processes. Immediately after the magnetization process start, the heat generation on the HTS tape begins to increase, while the cooling parameters are largely determined by the liquid forced movement speed and its effect on the boiling and heat transfer processes. The fluid velocity increase delays the onset of boiling, since the heat transfer from the surface is provided by the forced convection. A sharp heat generation on the sample leads to the refrigerant boiling, after which the thermal equilibrium establishing processes in the system and nitrogen boiling mode changing to convective begin. In this case, very rapid liquid mixing absence, characteristic of bubble boiling, leads to a sharp heat removal decrease and can lead to secondary overheating on the sample surface and reboiling. After the boiling start, forced convection continues to play a significant role, competing with heat transfer due to vaporization. As long as the liquid refrigerant is able to quickly remove the heat released on the HTS tape, a sharp increase in heat generation and losses on the sample does not occur. In the simulation, the absence of direct accounting of fluid motion and the formation of a bubble phase in LN_2 is compensated by the use of dynamic heat transfer coefficients for various liquid nitrogen boiling modes.

Thus, the choice of using one or another heat transfer coefficient depends on the temperature difference ΔT and heat flux into liquid nitrogen q and is set using the conditions "*if*". Since in some liquids, including liquid nitrogen, during the rapid heat flow growth the additional overheating may occur (boiling moment delay) by several degrees ΔT_{oh} (superheating), the liquid boiling temperature may exceed usual temperature onset bubble boiling delay value ΔT_{cb} (transition from convection to boiling). Therefore, the first type of "if" condition is fulfilled when the temperature difference ΔT reaches the liquid nitrogen overheating temperature ΔT_{oh}, which in general depends on the heater surface material and the boiling liquid properties. In our case ΔT_{oh} is assumed to be constant and equal to 3K. Immediately after ΔT_{oh} is reached, a developed bubble boil begins. When the heat flux decreases, the return from bubble boiling to convection does occur not at the temperature difference ΔT_{oh}, but at the temperature difference ΔT_{cb} (the second "if" conditions type), that is, there is a boiling hysteresis. ΔT_{cb} can be found from the condition of heat transfer coefficients equality in the natural convection and bubble boiling modes. Thus, the choice of heat transfer equation coefficients occurs automatically at each time step of the solution.

Liquid-free cooling is implemented in the form of a massive copper head, the heat sink of which corresponds to the power of a real cryocooler cooling system. In the case when the heat release of the sample is too large or the temperature dash is too sharp, and the power of the cryogenic system is insufficient for effective cooling, the temperature of the HTS element increases, which leads to a decrease in its current-carrying capacity. The model takes into account the possibility of degradation of the superconductor characteristics up to the complete loss of the trapped magnetic flux.

In order to preserve the real geometrical dimensions of all tape layers, when building a model, mesh drawing tools for the mesh of elements, converting a square mesh into a triangular at the individual domains boundaries, multiscale structuring and moving mesh tools were used.

3. Results and discussion

Complex electrodynamic and thermal calculations of a rotating bearing with an HTS stator were carried out. To validate the developed model, the horizontal and vertical load characteristics of the bearing in ZFC mode were measured. Measurements and calculations were carried out at the boiling point of liquid nitrogen.

The vertical displacement was measured as follows: the strain gauge abutted against rods against a textolite plate lying on a bearing, after which it shifted along the z axis until a predetermined value F_z was reached and vice versa. The bearing is displaced by 1 mm for every $\Delta F_z \sim 7.1$ N applied, up to $F_z \sim 45$ N. Thus, in essence, an experimental measurement of the bearing displacement from the applied force took place. The calculation of the levitation force from the vertical displacement of the magnetic assembly was also carried out (Fig. 2) and shows good agreement with the experimental data at the applied force of up to 45 N.

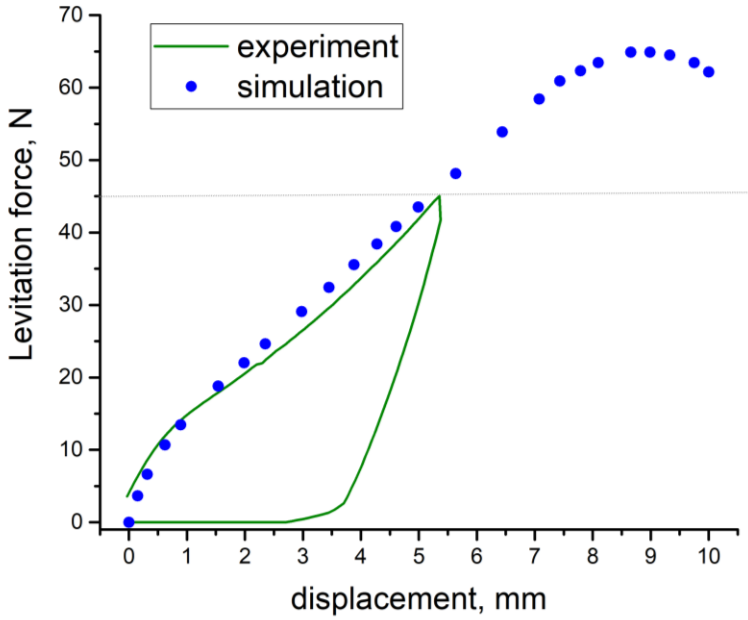

Figure 2. Bearing load curves for vertical displacement.

The calculations predict the possibility of the magnetic assembly displacing by a distance of 9 mm from the initial position, where the maximum value of the return force equal to 64 N is reached. The experimental verification of this fact is the subject of further research, since it requires some modification of the experimental setup.

For horizontal load measurements, the strain gauge was abutted against the bearing by a beam with a nozzle, after which it was shifted along the x axis and back by the same distance. The maximum distance the bearing was shifted in this case was 1.5 mm. The calculation results also demonstrate good agreement with experimental data (Fig. 3).

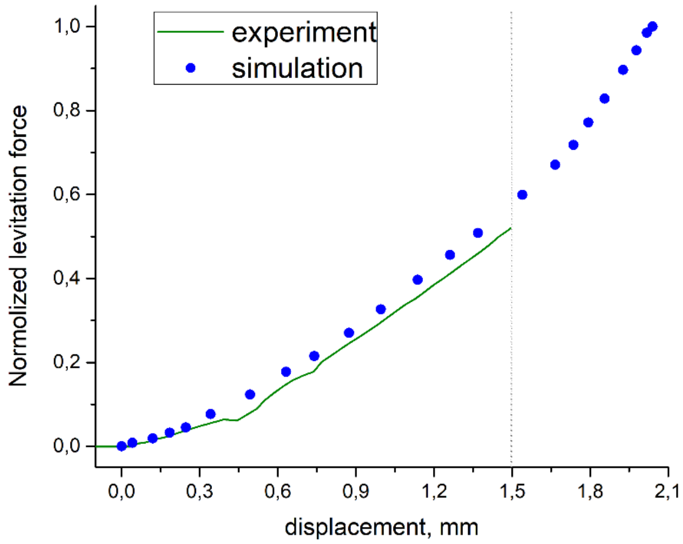

Figure 3. Bearing load curves at single horizontal displacement

Also, the calculations of the losses in the HTS tape superconducting layer resulting from the magnetization hysteresis during the bearing rotation in the inhomogeneous magnetic field (Fig. 4) were made. The calculation was performed for cooling to the several operating temperatures. It is worth noting that here we are talking only about the total hysteresis losses in superconducting layer, and not about the total losses for the HTS tapes in an alternating field, since total losses can include other contributions, such as losses in copper and other normal conductors. Calculation of total losses is the subject of the further research.

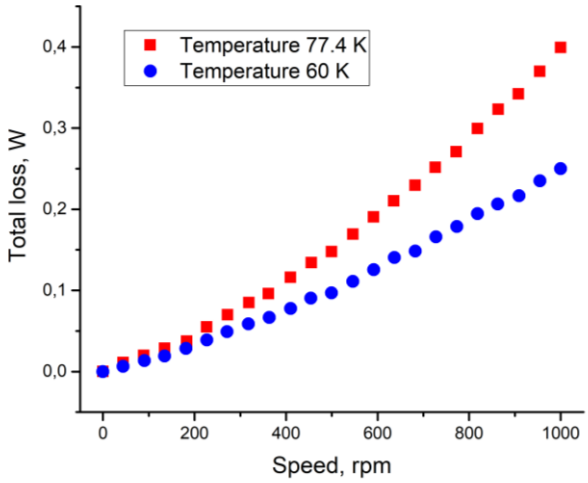

Figure 4. Dependence of AC losses on the rotation speed of a bearing with a HTS stator when working in an alternating field of the permanent magnets.

At a low speed (<200 rpm) a decrease of the temperature has practically no effect on the losses value, however, for high speed of rotation (>200 rpm), the difference is more than 60%. AC losses during operation of the bearing in an alternating magnetic field at higher revolutions are caused by fast remagnetization and as a result increase of heat generation in the superconducting tape. If the power of the cryogenic equipment is sufficient for the heat power evacuation the bearing will be able to work with the least losses and achieve high rotation speeds.

4. Conclusions

The calculation model based on the H-formalism for a rotating bearing with the HTS stator was developed using the Comsol Multiphysics software. The model takes into account the layered structure of superconducting tapes and the temperature dependence of the parameters for each SC tape layer. A feature of the developed model is a direct simulation of the motion of magnetic field sources during rotation of the rotor, consisting of an assembly of 48 permanent magnets (3 rows of 16 magnets 10 x 10 x10 mm^3 each) around the HTS stator. It was obtained load curves for the bearing at vertical and lateral displacement. Comparison of the theoretical and experimental data was carried out and demonstrated good agreement of the results.

The modeling predicts the maximum levitation force at the vertical displacement of 9 mm from the initial position at the vertical displacement and a monotonous increase in the levitation force at the lateral displacement until the HTS block and the magnetic assembly come into contact. In addition, the value of the hysteresis loss during the bearing rotation was calculated for the several operating temperatures. It is shown that the temperature decreasing is effective when the bearing is operating at higher speeds. The calculation of the total losses in the HTS tape is the subject of further research.

Thus, a numerical model applicable for the calculation of rotating systems was developed and verified. Since the parameters of individual magnetic levitation systems (MLS) are mainly individual for each specific design, numerical modeling is an indispensable tool for accurately calculating the current density (and, consequently, losses), levitation force and field distribution to develop the MLSs for various applications.

Acknowledgments
This work was supported by Russian Science Foundation (project 17-19-01527).

References

[1] Snitchler G, Gamble B, King C and Winn P, 2011 10 MW class superconductor wind turbine generators *IEEE Trans. Appl. Supercond.* **21**, no. 3, pp. 1089-1092,
[2] Huang Z *et.al.* 2016 Study of the pulsed field magnetization strategy for the superconducting rotor *IEEE Trans. Appl. Supercond.* **26**, no. 4, pp. 1-5,
[3] Rong C C and Barnes P N 2017 Developmental Challenges of SMES Technology for Applications *IOP Conf. Ser. Mater. Sci. Eng.* **279** 012013
[4] Irina A Sergei P Igor R and Maxim O 2019 Modeling of magnetization and levitation force of HTS tapes in magnetic fields of complex configurations *Superconductor Science and Technology* **32**, no. 10, p. 105001.
[5] Fujishiro *et al.* 1994 Anisotropic thermal diffusivity and conductivity of YBCO(123) and YBCO(211) mixed crystals *Jpn. J. Appl. Phys*. **33**, part 1, no. 9A, pp. 4965-4970
[6] Bonura M and Senatore C 2014 High-field thermal transport properties of REBCO coated conductors *Supercond. Sci. Technol.* **28** 025001
[7] Ahlers G 1965 Heat capacity of Copper *Rev. Sci. Instrum.* **37**, issue 4, pp. 477- 480
[8] Matula R A 1979 Electrical resistivity of copper, gold, palladium, and silver *J. Phys.Chem. Ref. Data* **8**, no. 4, pp. 1147-1298
[9] Smith D R and Fickett F R 1995 Low-temperature properties of silver *J. Res. Natl.Inst. Stand. Technol.***100**, no. 2, pp. 119-171
[10] http://www.htsmodelling.com/?page_id=1039
[11] Zou S, Zermeño V M R and Grilli F 2016 Simulation of stacks of high-temperature superconducting coated conductors magnetized by pulsed field magnetization using controlled magnetic density distribution coils *IEEE Trans. Appl. Supercond.***26**, no. 3, pp. 8200705
[12] Ming-Heng S, Ma J and Bu-Xuan W 1993 Analysis on hysteresis in nucleate pool boiling heat transfer International *Journal of Heat and Mass Transfer* **36** 4461-6
[13] Stephan K and Abdelsalam M 1980 Heat-transfer correlations for natural convection boiling

International Journal of Heat and Mass Transfer **23** 73-87
[14] Fetisov S s, Vysotsky V and Zubko V V 2011 HTS Tapes Cooled by Liquid Nitrogen at Current Overloads *Applied Superconductivity, IEEE Transactions on* **21** 1323-7